Supporting Information

Bimetallic Synergistic Effect on the Atomic-scale of the Defect-enriched NiV-Layered Double Hydroxide Nanosheets for Electrochemical Phenol Hydroxylation

Guangyao Li,[‡a] Yanqi Xu,[‡*acd] Hong Pan,[b] Xiangli Xie,[b] Rongrong Chen,[a] Di Wu,[a] and Linjiang Wang*[acd]

[a] College of Materials Science and Engineering, Guilin University of Technology, Guilin 541004, China;

[b] College of Chemistry and Bioengineering, Guilin University of Technology, Guilin, 541004, China;

[c] Key Laboratory of New Technology for Processing Nonferrous Metals and Materials, Ministry of Education, Guilin University of Technology, Guilin 541004, China;

[d] Collaborative Innovation Center for Exploration of Hidden Nonferrous Metal Deposits and Development of New Materials in Guangxi, Guilin University of Technology, Guilin 541004, China;

‡ These authors contributed equally to this work.

* Corresponding author, E-mail: xuyanqi@glut.edu.cn; wlinjiang@163.com

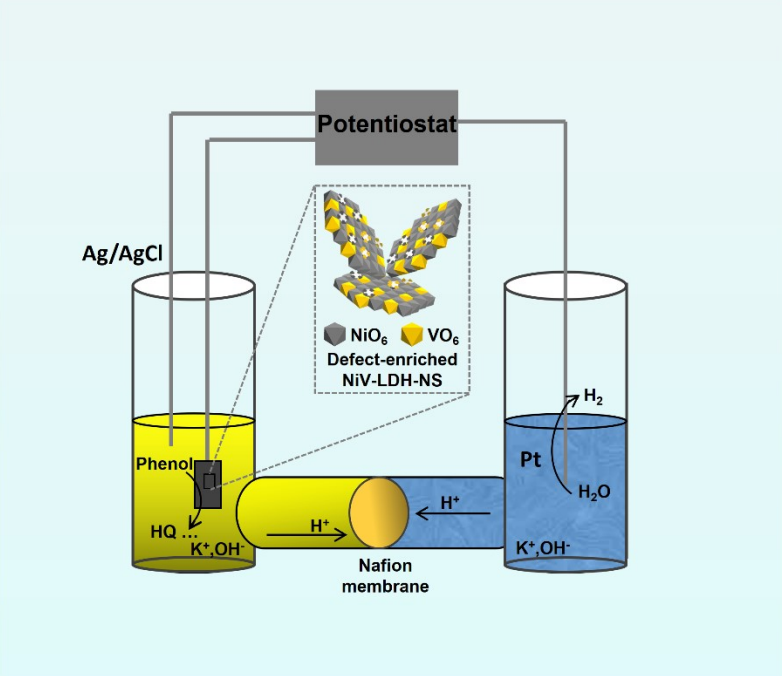

Scheme S1 The chemicals-energy co-generation system.

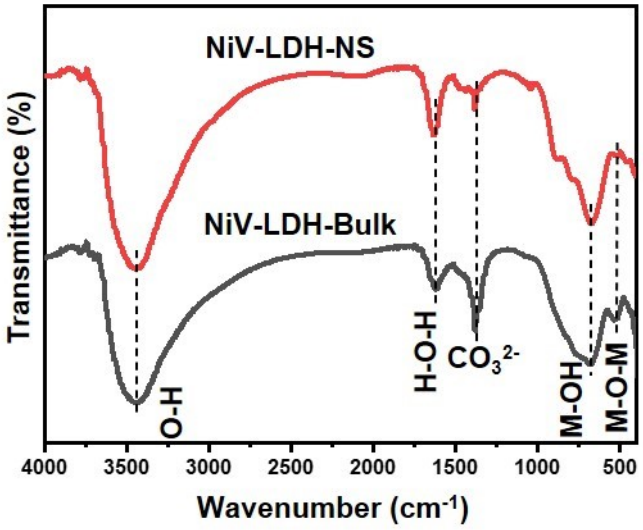

Fig. S1 FTIR spectra of NiV-LDH-NS and NiV-LDH-Bulk.

The spectra of NiV-LDH showed a sharp absorption band with a center at ~ 1350 cm^{-1} assigned to the interlayer CO_3^{2-} anions. Broad absorptions located at ~ 3500 cm^{-1} and ~ 1650 cm^{-1} were assigned to the O-H stretching and bending vibration of interlayer water molecules, respectively. The absorption peaks at ~ 680 cm^{-1} and ~ 510 cm^{-1} were attributed to the vibrations of metal-O and metal-O-metal bonds, respectively.

Table S1 Unit cell parameters of NiV-LDH-NS and NiV-LDH-Bulk.

Entry	Sample	$2\theta_{(110)}$	$d_{(110)}$ [Å]	a [Å]	Strain degree around (110) direction
1	NiV-LDH-NS	61.36	1.51	3.02	-3.87%
2	NiV-LDH-Bulk	60.03	1.54	3.08	0%

Table S2 Comparison of physicochemical properties of NiV-LDH-NS and NiV-LDH-Bulk.

Entry	Sample	Surface area (m^2g^{-1})	Pore size (nm)	Pore volume (cm^3g^{-1})
1	NiV-LDH-NS	239.97	3.68	0.22
2	NiV-LDH-Bulk	22.10	5.22	0.03

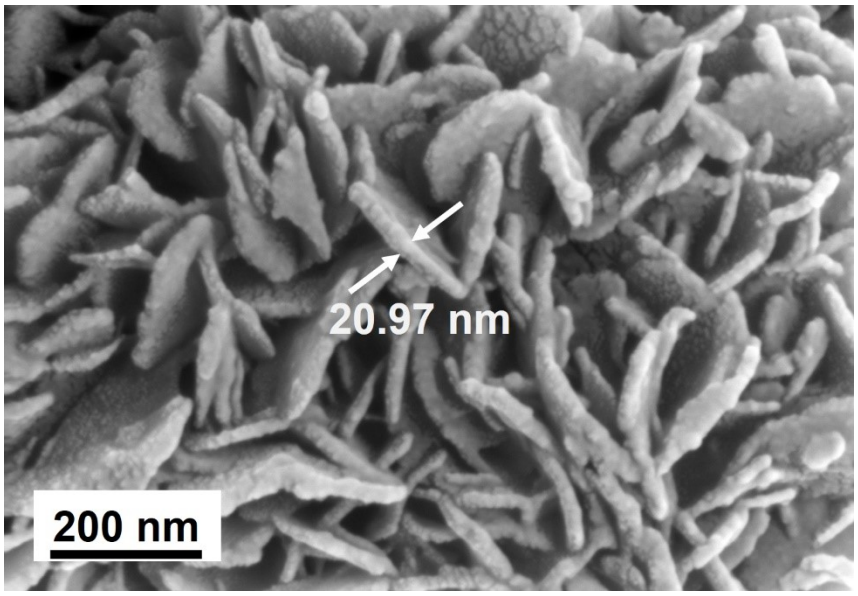

Fig. S2 SEM image of NiV-LDH-Bulk.

Table S3 Summary of elemental analysis date for NiV-LDH-NS and NiV-LDH-Bulk from ICP-AES results.

Entry	Sample	Ni (mM)	V (mM)	$Ni_xV_y(OH)_2(CO_3)_z \cdot nH_2O$
1	NiV-LDH-NS	15.59	3.62	$Ni_{0.802}V_{0.198}(OH)_2(CO_3)_{0.084} \cdot 0.828H_2O$
2	NiV-LDH-Bulk	15.38	3.69	$Ni_{0.807}V_{0.193}(OH)_2(CO_3)_{0.096} \cdot 0.835H_2O$

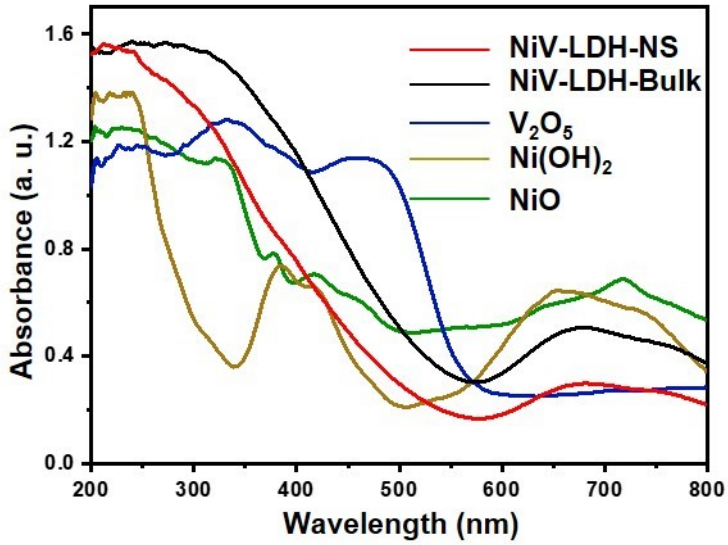

Fig. S3 UV-vis diffuse reflectance spectroscopy of NiO, $Ni(OH)_2$, V_2O_5, NiV-LDH-Bulk and NiV-LDH-NS, respectively.

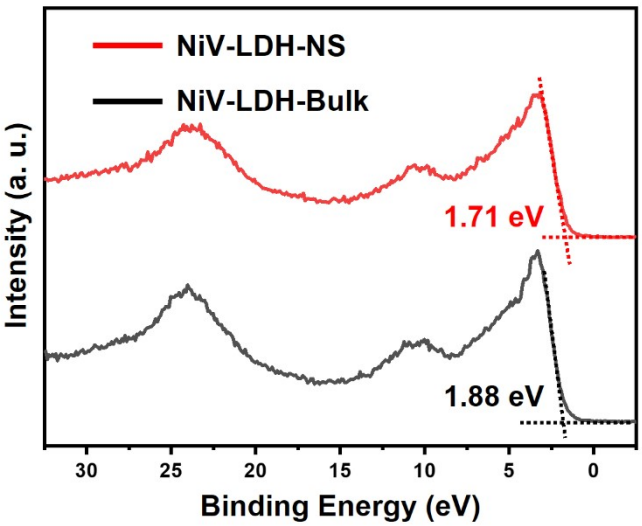

Fig. S4 Valance band XPS spectra of NiV-LDH-NS and NiV-LDH-Bulk.

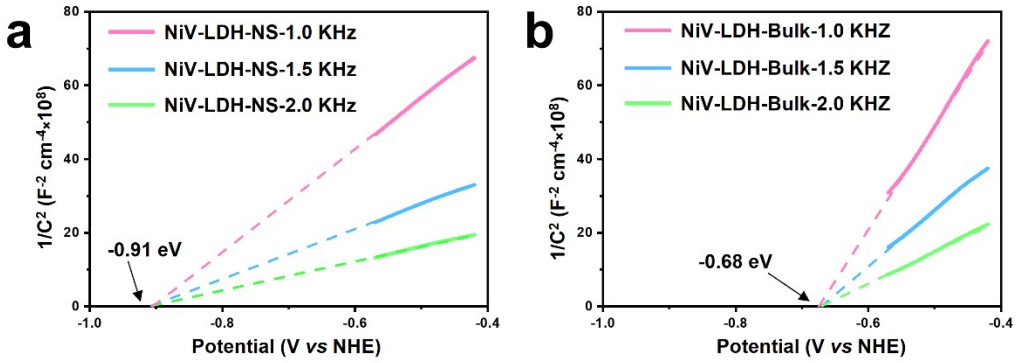

Fig. S5 Mott-Schottky plots of (a) NiV-LDH-NS and (b) NiV-LDH- Bulk.

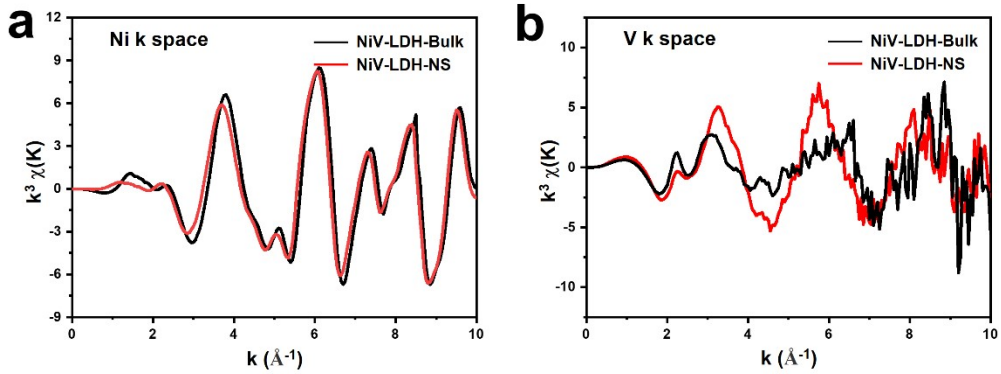

Fig. S6 (a) Ni and (b) V K-edge EXAFS oscillation functions k^3 χ (k) of NiV-LDH-NS and NiV-LDH-Bulk.

Table S4 Local structure parameters around Ni estimated by EXAFS analysis.

Sample	Shell	*N*[a]	*R* [Å][b]	σ^2 [Å^2][c]
NiV-LDH-Bulk	Ni-O	6.0	2.06	0.0065
	Ni-Ni/V	6.0	3.10	0.0073
NiV-LDH-NS	Ni-O	5.4	2.06	0.0066
	Ni-Ni/V	5.6	3.10	0.0076

[a] *N* = coordination number; [b] *R* = distance between absorber and backscatter atoms; [c] σ^2 = Debye-Waller factor.

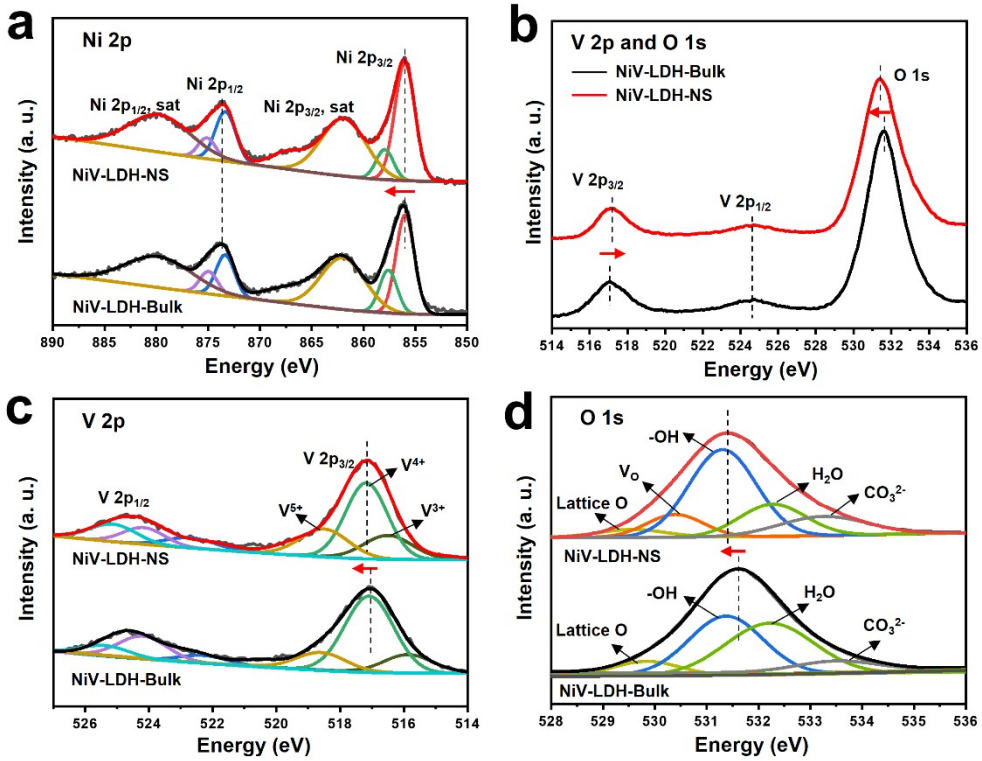

Fig. S7 XPS spectra of NiV-LDH-Bulk and NiV-LDH-NS.

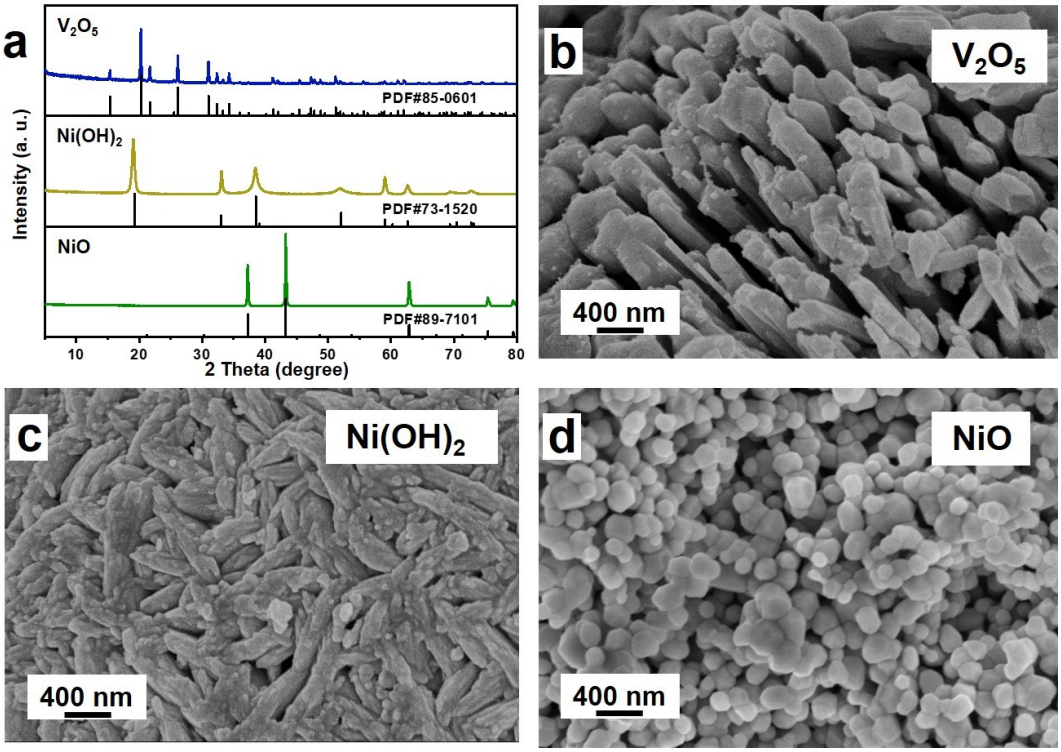

Fig. S8 XRD patterns and SEM images of V_2O_5, $Ni(OH)_2$ and NiO, respectively.

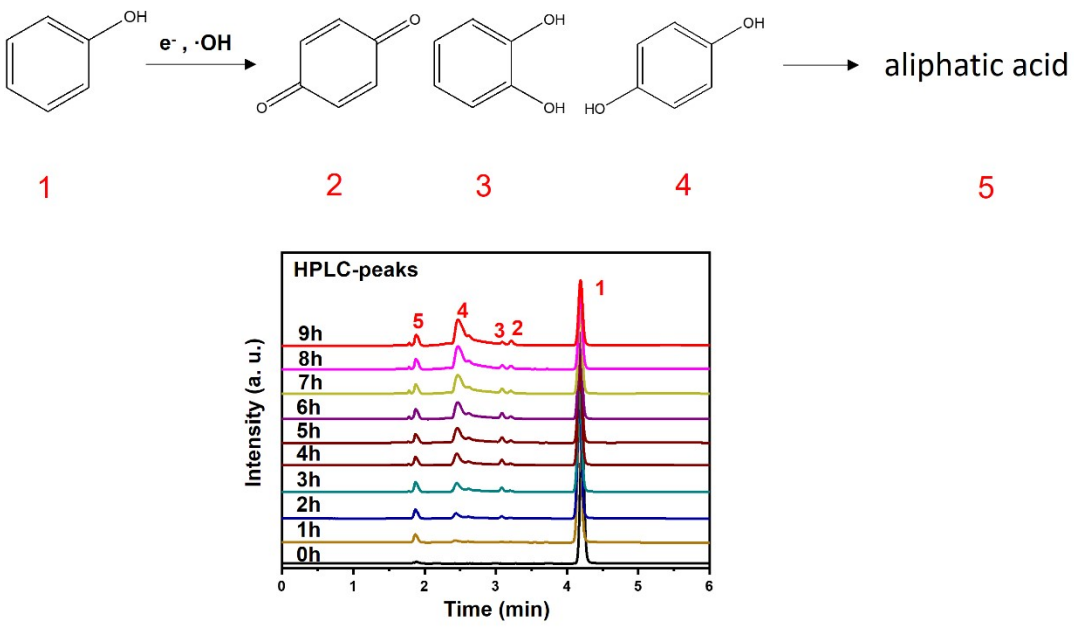

Fig. S9 The procedure of electrochemical phenol hydroxylation over NiV-LDH-NS.

The main peaks seen in the Fig. S9 were marked for the electrocatalytic products, which corresponding to phenol (peak 1), benzoquinone (peak 2), catechol (peak 3), hydroquinone (peak 4), and aliphatic acid (peak 5).

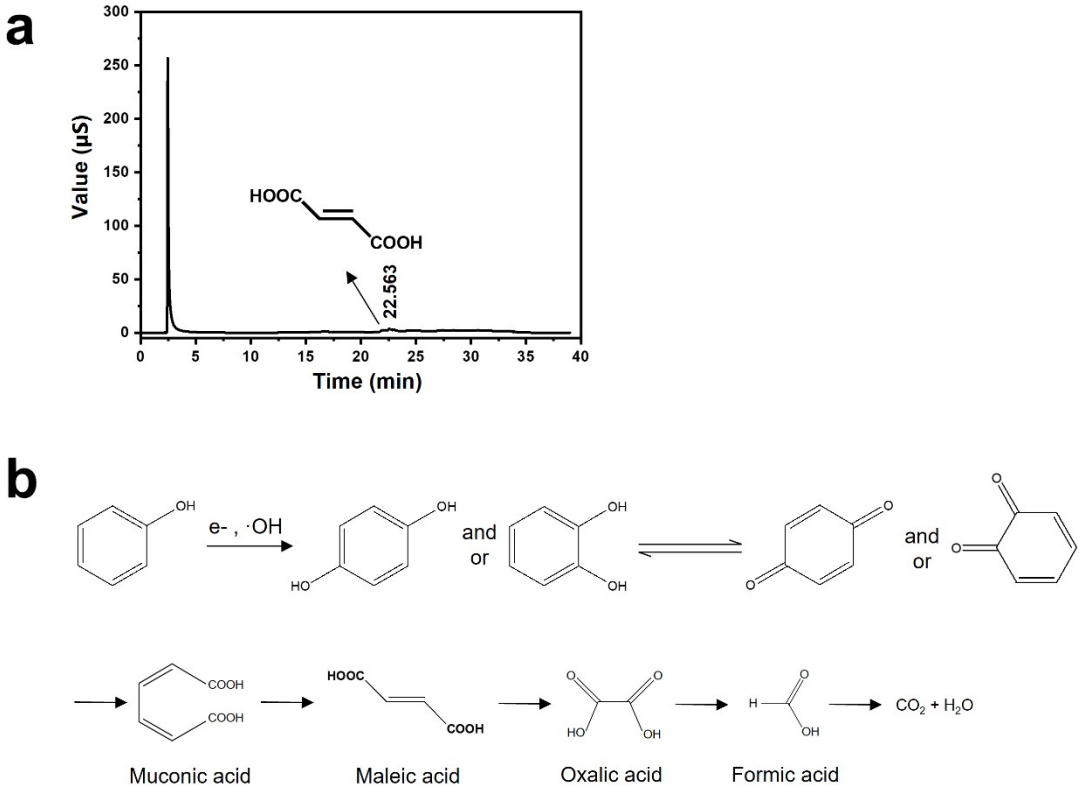

Fig. S10 (a) The ion chromatography of the electrocatalytic products of phenol for NiV-LDH-NS electrocatalyst in 9 h. (b) The degradation process of phenol.

Table S5. Comparison of phenol hydroxylation activity with different chemical methods.

Catalyst	Reaction Condition	Oxidation Agent	Solvent	Phenol Conversion	Product Selectivity	Ref.
Fe-ESP	37 °C	H_2O_2	acetonitrile	25%	17% (CAT) 8% (HQ)	39
Fe_3O_4 @CuMgAl	65 °C	H_2O_2	H_2O	29.8%	64.4% (CAT) 34.5% (HQ)	40
Cr-MOF-199	70 °C	H_2O_2	acetonitrile	71%	35% (CAT) 20% (HQ)	2
GO-Cu-SiO_2-SA	70 °C	H_2O_2	H_2O	90%	60% (CAT) 40% (HQ)	41
NiFe-LDH	Xe lamp 550 nm	H_2O_2	H_2O	40%	69% (CAT) 30% (HQ)	23
NiV-LDH-NS	0.5V *vs* Ag/AgCl	H_2O	H_2O	72%	HQ (71%)	This work

CAT: catechol, HQ: hydroquinone.

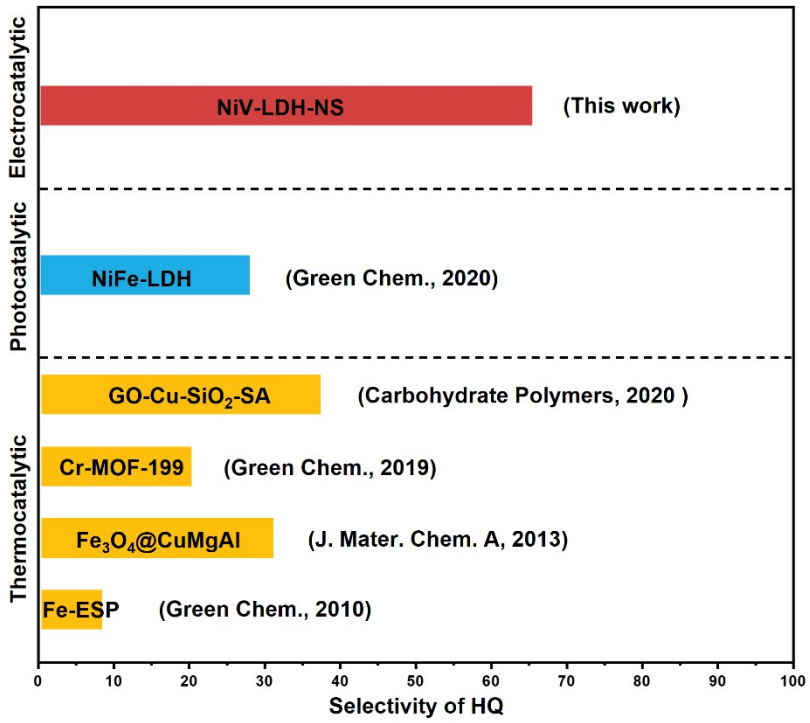

Fig. S11. Selectivity of HQ compared to different reported catalyst.

Table S6. Comparison of phenol hydroxylation activity with the industrial process.

Catalyst	Reaction Condition	Oxidation Agent	Solvent	Phenol Conversion	Product Selectivity	Recycle	Ref.
TS-1	70–100 °C	H_2O_2 (30–50 wt%)	acetone or methanol	20–25%	DHB (90–95%)	–	42
NiV-LDH-NS	0.5V *vs* Ag/AgCl	H_2O	H_2O	72%	HQ (71%)	√	This work

DHB: dihydroxybenzenes (catechol and hydroquinone), HQ: hydroquinone.

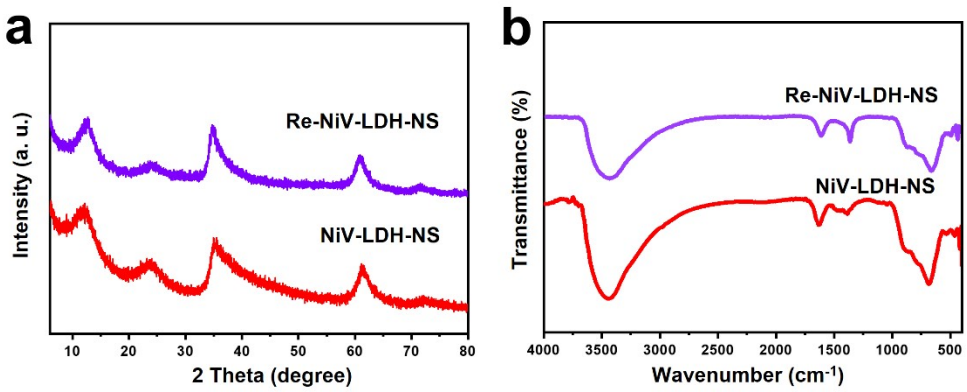

Fig. S12 (a) XRD patterns and (b) FTIR spectra of NiV-LDH-NS and Re-NiV-LDH-NS.

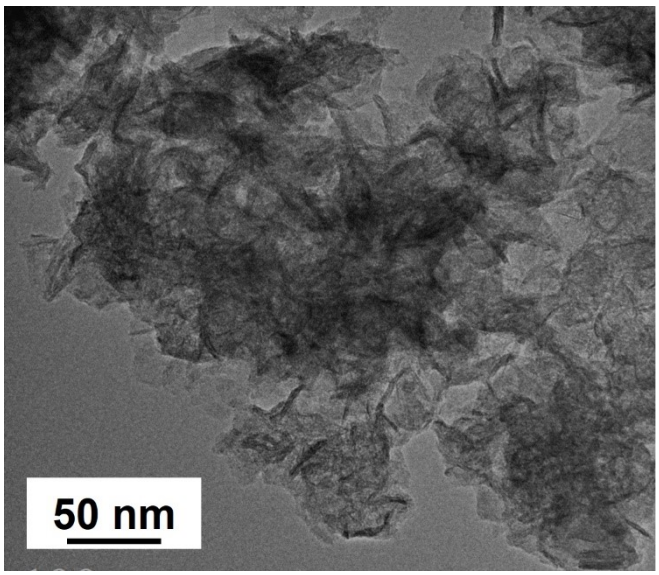

Fig. S13 HRTEM image of Re-NiV-LDH-NS.

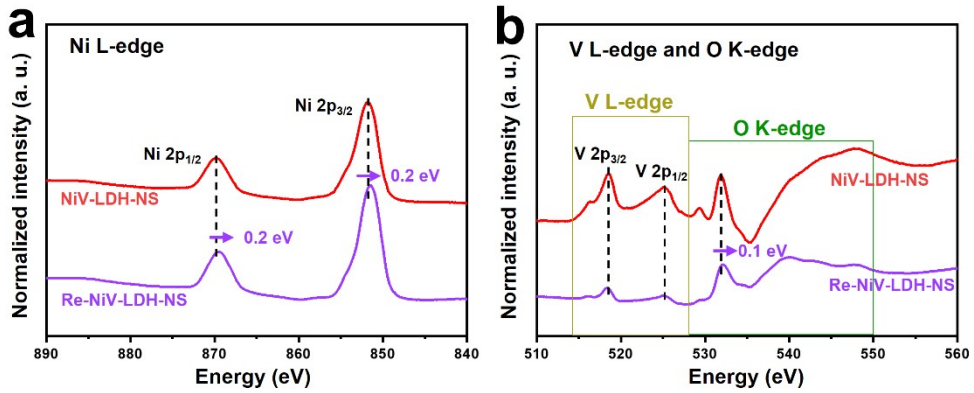

Fig. S14 XAS spectra of Re-NiV-LDH-NS (purple) and NiV-LDH-NS (red), respectively.

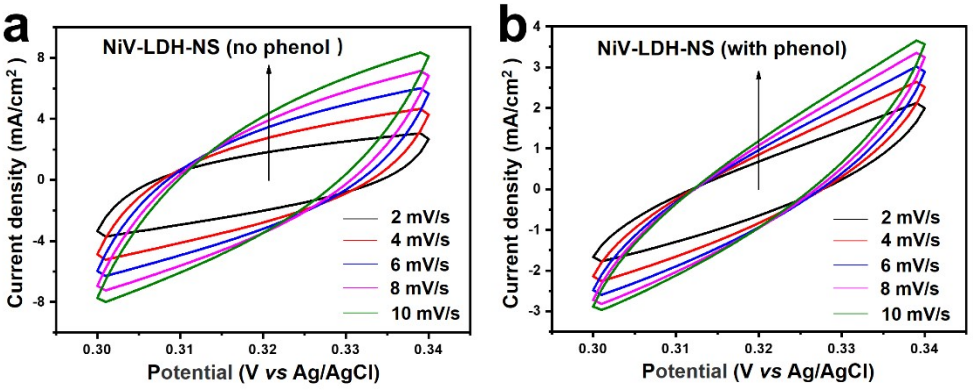

Fig. S15 CV curves of NiV-LDH-NS for (a) water oxidation and (b) phenol hydroxylation.

To further understand the reason behind the high catalytic performance of NiV-LDH-NS with and without phenol, electrochemical active surface areas (ECSA) were obtained from cyclic voltammetry (CV) curves in 1 M KOH and compared. It was well known that the increase of ECSA often leaded to enhancement of the catalytic activity. Fig. S15 showed typical CV curves of 0.3 ~ 0.34 V *vs* Ag/AgCl with different scan rates. By plotting the ΔJ at 0.32 V *vs* Ag/AgCl against the scan rate, the linear slope that was twice the double layer capacitance (C_{dl}) could be obtained and was normally used to represent the corresponding ECSA.

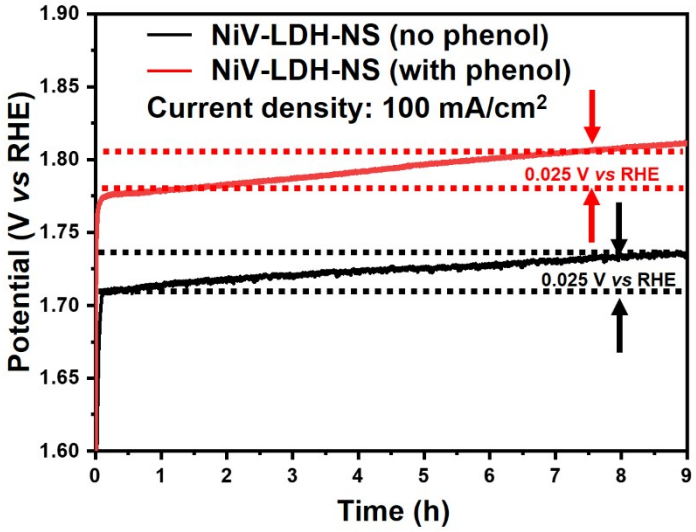

Fig. S16 The chronoamperometry experiments of NiV-LDH-NS with and without 10 mM phenol at the current density of 100 mA cm^{-2}.

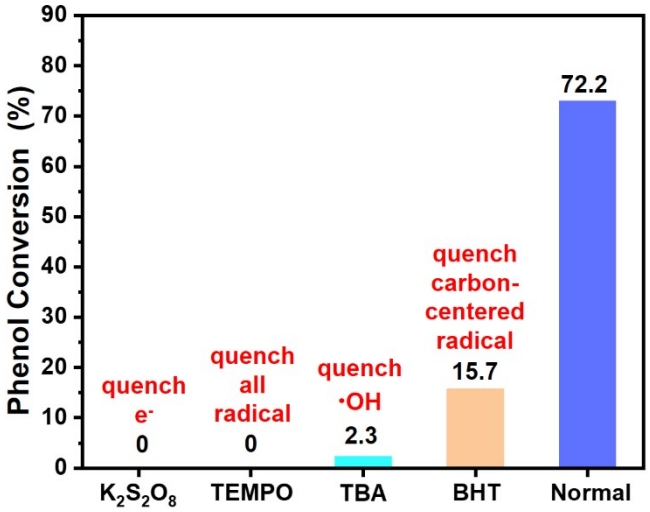

Fig. S17 The conversion of phenol hydroxylation in the addition of various scavengers respectively. Reaction condition: NiV-LDH-NS 20 mg, 40 °C, onset potential 0.5 V *vs* Ag/AgCl, and reaction time 9 h.